Structures and Mechanical Properties of Zone-Drawn–Zone-Annealed Blends of Cocrystallizing Poly(butylene terephthalate) and a Poly(ether ester)

A. A. APOSTOLOV,[1] M. EVSTATIEV,[1] S. FAKIROV,[2,*] A. KLOCZKOWSKI,[3,†] and J. E. MARK[3]

[1]Laboratory on Structure and Properties of Polymers, Sofia University, 1126 Sofia, Bulgaria; [2]Bogazici University, Polymer Research Center, Chemical Engineering Department and TUBITAK Advanced Polymeric Materials Research Center, 80815 Bebek-Istanbul, Turkey; [3]The University of Cincinnati, Department of Chemistry and Polymer Research Center, Cincinnati, Ohio 45221-0172

SYNOPSIS

Poly(butylene terephthalate) (PBT) and a poly(ether ester) (PEE) based on PBT and poly(ethylene glycol) were melt-blended and extruded as films with quenching. They were then zone-drawn (ZD) and zone-annealed (ZA) at various stresses (between 10 and 50 MPa) at temperatures of 160 and 190°C. The goal was to improve their mechanical properties relative to those of the same blend, but cold-drawn ($\lambda = 5$) and isothermally annealed with fixed ends at the same temperatures for 6 h. All samples were characterized by DSC, WAXS, SAXS, and static mechanical property measurements. In contrast to the isothermally annealed samples, the zone-drawn and zone-annealed ones exhibit one population of crystallites arising from the homo-PBT, as demonstrated by the DSC and SAXS measurements. In addition, however, the WAXS photographic patterns indicate that zone annealing at 190°C results in isotropization of crystallites originating from the PEE, resulting in the formation of a microfibrillar-reinforced composite. It is assumed that some of the isotropic crystallization occurs on preexisting homo-PBT crystallites, i.e., a partial cocrystallization occurs, improving the adhesion between the components of the blend. The structural features created in the zone-drawn–zone-annealed materials result in higher values of the Young's modulus and tensile strength in comparison to the materials receiving the simple isothermal treatment (1,200 vs. 480 MPa and 213 vs. 113 MPa, respectively). © 1996 John Wiley & Sons, Inc.

INTRODUCTION

Polymer blends show increasing commercial importance as high-performance materials, currently constituting over 30% of the polymer market.[1] However, the blending of two polymers usually results in immiscibility which generally makes it necessary to incorporate a third component (i.e., a compatibilizer such as a copolymer).[2–4] An alternative way for overcoming the immiscibility is to establish chemical bonds between the components, using either inherently present functional groups (in case of condensation polymers) or introducing such groups onto other types of polymers before their blending (in the case of polyolefins).[1] A special example of the creation of relatively strong bonds (via tie molecules) between components in a blend is cocrystallization. This approach is particularly suitable for blends of a crystallizable homopolymer with a block copolymer, providing that one of the blocks has the same structure as that of the homopolymer.

Soon after the development of poly(ether esters) (PEE) based on poly(butylene terephthalate) (PBT) and poly(tetramethylene oxide) (PTMO), an attempt to change their properties by addition

* To whom correspondence should be addressed at Laboratory on Structure and Properties of Polymers, Sofia University, 1126 Sofia, Bulgaria.

† Present address: Laboratory of Theoretical Biology, National Cancer Institute, National Institutes of Health, Bethesda, MD 20205.

Journal of Applied Polymer Science, Vol. 59, 1667–1675 (1996)
 CCC 0021-8995/96/111667-09

of homo-PBT was made.[5] The resulting blend, having the same overall PBT content as a certain PEE, was grossly different from the latter. Both the flexibility and the impact strength at low temperatures were improved.

Recently, Gallagher et al.[6] demonstrated that cocrystallization occurs in blends of PBT and a PEE based on PBT and PTMO when the PBT content in the PEE is between 75 and 91 wt %. They did not report, however, on cocrystallization in blends containing PEE having less than 75 wt % PBT. Also relevant is a study[7] on melt-blended, cold-drawn, and isothermally annealed PBT with PEE based on PBT and poly(ethylene glycol) (PEG) which showed that partial cocrystallization occurs. The cocrystallization in this particular case can be considered as "epitaxial" growth[6] of PBT crystallites, arising from the PEE onto homo-PBT crystallites, i.e., there was the formation of continuous PBT crystals consisting of two crystallographically identical populations of crystallites, not spatially separated, but differing in size, degree of perfection, origin, and time of appearance. In contrast to this partial cocrystallization, complete cocrystallization (the formation of uniform crystallites with simultaneous participation of PBT from both the homo-PBT and the PEE) requires sufficiently long PBT sequences in the PEE for formation of lamellar thickness typical of homo-PBT crystallites. This last requirement for complete cocrystallization is not fulfilled for PEE containing less than 75 wt % PBT, due to the insufficient length of the PBT hard segments, as shown in a previous study.[8] Of primary importance is the fact that even partial cocrystallization contributes to the improvement of the adhesion between the components (in the present case, homo-PBT and the PEE copolymer).

Another peculiarity of the blend under investigation is its ability to form microfibrillar-reinforced composites (MFC) due to the different melting points of the crystallites arising from the two components. As shown for other blends of condensation polymers,[9–13] the microfibrils can be created during MFC manufacturing by drawing the polymer blend, which leads to orientation of both components (fibrillization), followed by melting of the low-melting component (isotropization) with preservation of the oriented microfibrillar structure of the higher-melting component. It is important to note that, in addition to isotropization during short thermal treatment, chemical reactions (additional condensation and transreactions) between condensation polymers (in the melt[14] as well as in the bulk solid state[15]) take place at the interfaces. The resulting copolymeric interphase plays the role of a self-compatibilizer. To follow the compatibilizing contribution from only the partial cocrystallization, an attempt was made to avoid the occurrence of transreactions by choosing appropriate temperatures and durations of the treatment.

The purpose of the present study was to find a way for improving the mechanical properties of PBT/PEE blends, for which it has already been demonstrated that incompatibility can be overcome to some extent by means of partial cocrystallization of PBT sequences from the two components.[7] This was observed on samples drawn at room temperature and annealed for a relatively long time (6 h) at constant length. Better mechanical properties are attempted in the present case by increasing both orientation and crystalline order by means of zone drawing and zone annealing[16] as well as treatment duration. This should lead to formation of MFC and the occurrence of cocrystallization. In comparison to the other approaches for effective polymer orientation, such as cold drawing (CD) or hot drawing[17,18] with isothermal annealing (IA), solid-state extrusion,[17–19] and rapid drawing from the melt or from solutions,[17,20,21] the zone-drawing and zone-annealing approach is known to lead to the most significant improvements in mechanical properties.[16]

EXPERIMENTAL

The PBT employed was a commercial sample that was kindly supplied by the DuPont Co. ("RE 6131", $\bar{M}_n$ = 21,300 g/mol). The PEE was prepared in a semicommercial scale[22] using PEG of molecular weight 1000 g/mol and having a PBT/PEG wt ratio of 49/51. Both the PBT and PEE were cooled in liquid nitrogen, finely ground, and then mixed in a ratio of PBT/PEE = 51/49 wt % to produce the blend containing a total amount of 75 wt % PBT. Films of the blend were prepared according to the following procedure: A capillary rheometer, flushed with argon and heated to 225°C, was loaded with the dried powdered material. The melt obtained was kept in the rheometer for 5 min and then extruded through the capillary (diameter 1 mm) onto closely spaced metal rolls immersed in liquid nitrogen and rotating at 30 rpm. The films obtained were 3–4 mm wide and 0.1–0.15 mm thick, depending on the extrusion rate and the distance between the rolls. Thereafter, the films were zone-drawn (ZD) and zone-annealed (ZA) according to the following procedure: The films, as quenched, were subjected to heating by means of a narrow heating device (glass

tube of diameter 3 mm) attached to the crosshead of a Zwick 1464 machine. The heater was moved from the lower to the upper part of the sample under tension at a crosshead speed of 50 mm/min. The values of the stress, temperature, number of heater passages, and the draw ratios used are given in Table I, along with the sample designations.

Values of the glass-transition temperature T_g and the crystallization parameters of the samples were obtained using a Mettler T3000 thermoanalyzer over the temperature range −100 to 300°C, at a heating rate of 10°C/min in an argon atmosphere. Liquid nitrogen was applied for subambient cooling and calibration was done with an indium standard. The sample size was 15–20 mg and the reported values of T_g were taken to be midpoint values determined from a single heating run. The PBT degree of crystallinity w^{PBT} was estimated from the experimentally obtained heat of fusion ΔH relative to the heat of fusion of the fully crystalline PBT (ΔH_0 = 144.5 kJ/kg)[23] and the relative amount of PBT in the blend (0.75):

$$w^{PBT} = \frac{\Delta H}{0.75\Delta H_0} \quad (1)$$

The mechanical tests were carried out at room temperature in a static mode using a Zwick 1464 apparatus equipped with an incremental extensiometer at a crosshead speed of 5 mm/min. Initial lengths were typically 50 mm. Values of the Young's modulus E, tensile strength σ, and relative deformation at break ε were evaluated from the resulting stress–strain curves. All values were averaged from four measurements.

Wide-angle X-ray scattering (WAXS) measurements were carried out on a Siemens D500 diffractometer, and small-angle X-ray scattering (SAXS) data were taken with a Kratky camera. Ni-filtered CuKα radiation was used in both cases. The dimensions of the PBT crystallites in the respective directions were calculated from the half-widths of the (010), (100), and ($\bar{1}$04) reflections using Scherrer's formula. Azimuthal scans of the ($\bar{1}$04) reflection from −36° to 36° were used for qualitative evaluation of the crystallite orientation in the axial direction. As this reflection is very weak, these scans were taken step by step in a preset time mode with an increment of 4°. The long spacing L was calculated from the angular position of the maximum in the SAXS curves by means of Bragg's law. Photographic wide-angle X-ray patterns were taken using a flat camera.

RESULTS

Structural Characterization

Figure 1 shows the thermograms for the samples described in Table I, along with those of two samples of the same blend, but drawn at room temperature and subsequently annealed at constant length. The corresponding numerical data are summarized in Table II. For the ZD–ZA samples A–F (Table I), two well-pronounced glass transition temperatures are seen in almost all the thermograms. The low-temperature one (~ −40°C) originates from the PEG, whereas the high-temperature one (~ 40°C), from the PBT (Fig. 1, curves A–F). In contrast to the blends of immiscible homopolymers, the existence of two glass transition temperatures (T_g^{PBT} and T_g^{PEG}) in this case is a result of an inherited property of the block copolymer PEE, for which the same transitions were reported for the unblended, neat state.[22] These glass transition temperatures cannot be seen for the CD–IA samples (curves G and H), probably due to the much lower amount present (approximately 3 against 15 mg for samples A–F).

Table I Values of the Treatment Stress P, Annealing Temperature T_a, Number of Crosshead Passages N, and Draw Ratio After the Respective Preparation Steps λ_1, λ_2, and λ_3

	Zone Drawing				Zone Annealing							
Sample Designation	P (MPa)	T_a (°C)	N	λ_1	P (MPa)	T_a (°C)	N	λ_2	P (MPa)	T_a (°C)	N	λ_3
A	10	160	1	3.8	30	160	1	4.0	—	—	—	—
B	10	160	1	3.8	30	160	1	4.0	50	160	4	4.4
C	10	160	1	3.8	30	160	1	4.0	50	190	4	5.9
D	10	190	1	4.2	30	190	1	4.5	—	—	—	—
E	10	190	1	4.2	30	190	1	4.5	50	160	4	4.6
F	10	190	1	4.2	30	190	1	4.5	50	190	4	5.2

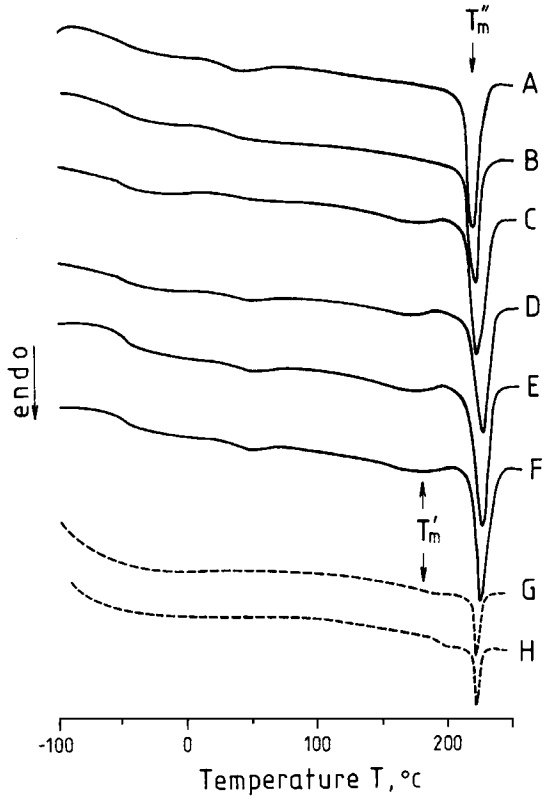

Figure 1 DSC curves of the blend PBT/PEE (51/49 wt %) subjected to the ZD–ZA and CD–IA treatments at constant length. For sample designations (A–F), see Table I; samples G and H had been isothermally annealed for 6 h at 170 and 190°C, respectively.

For a neat sample of PEE with the composition of PBT/PEG = 49/51 wt %, melting of the PEG crystals occurs at about 0°C.[24] Although the same PEE was used in the blending, no melting of PEG crystals could be detected from the curves presented in Figure 1. This is probably due to the significantly lower PEG content in the blend, as well as to the expected inhibition effect of the homo-PBT on the crystallization of PEG blocks (which even in neat PEE is weak and hard to detect[24]).

The next well-resolved transition temperature in the thermograms is the PBT glass transition temperature, T_g^{PBT}. It is about 40°C for all the samples. The observation of two glass transition temperatures, T_g^{PEG} and T_g^{PBT}, clearly demonstrates the existence of two spatially well-separated amorphous phases. The first comprises the total PEG amount, and the second, the amorphous parts of both the homo-PBT and the PBT from the PEE. In addition to these two amorphous phases, there is unambiguous evidence for the existence of a third crystalline phase, as can be seen on thermograms A–H in Figure 1. The very sharp peaks located at 225°C reflect the melting behavior of the crystallites arising from homo-PBT, as shown previously.[7] This T''_m peak is preceded by another very flat one (T'_m in Fig. 1), located at around 180°C (samples C–F), 190°C (sample G), or 200°C (sample H). This melting peak can be related to the PBT crystals originating from the PEE by means of curves G and H. The difference in the low-temperature peak for zone-treated samples (curves C–F) and the isothermally treated samples (curves G and H) may be related to the significant difference in the treatment time: a couple of minutes in the first case vs. 6 h in the second.[7]

Finally, it should be noted that the observed transition temperatures, T_g and T_m, do not depend on treatment conditions during the zone drawing and zone annealing (described in Table I), as can readily be seen from the numerical values summarized in Table II.

Further structure characterization was carried out using wide-angle and small-angle X-ray scattering. Figure 2 shows the SAXS curves for all the ZD–ZA samples, together with two curves for blends that had been isothermally annealed at a fixed length, replotted from the previous study[7] for purposes of comparison. All the curves for the ZD–ZA samples are very similar and consist of one well-developed maximum (Fig. 2, samples A–F), whereas the samples annealed with fixed ends reveal one broad maximum (G) or a plateau (H), which may be considered as a overlapping of two differing in angular position maxima. As concluded previously,[7] these latter two curves are representative of two populations of PBT crystallites arising from the two components and embedded in a matrix which creates two different periodicities (long spacings). In the case of the ZD–ZA samples (Fig. 2, curves A–F), only one long spacing of about 140 Å can be detected, which in-

Table II Glass Transition Temperatures T_g^{PEG} and T_g^{PBT}, PBT Melting Temperatures T'_m and T''_m, and Degrees of PBT Crystallinity w^{PBT} for ZD–ZA Treatment

Sample	T_g^{PEG} (°C)	T_g^{PBT} (°C)	T'_m (°C)	T''_m (°C)	w^{PBT}
A	−47	40	—	224	0.16
B	−43	38	—	226	0.19
C	−44	43	176	228	0.21
D	−44	43	177	225	0.20
E	−45	43	178	226	0.20
F	−44	44	176	228	0.20

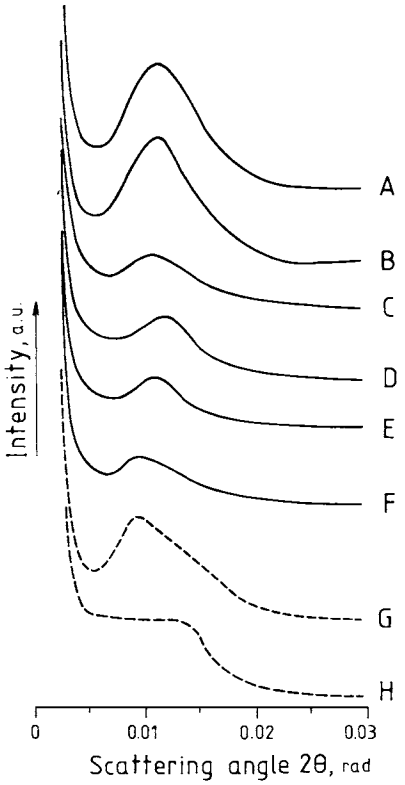

Figure 2 SAXS curves of the blends subjected to the ZD–ZA and CD–IA treatments at constant length. For sample designations, see Figure 1.

dicates that the PBT crystallites from the PEE have the same distribution as those of homo-PBT. This is probably due to the small proportion of this population, as can be concluded from the DSC measurements (Fig. 1, curves C–F). Some of these crystallites are presumably partially cocrystallized, i.e., grown onto the surface of the preexisting PBT crystallites of the homopolymer.

Table III lists the two lateral crystallite sizes D_{010} and D_{100} [measured in directions normal to the (010) and (100) planes] and the longitudinal size $D_{\bar{1}04}$ (which corresponds approximately to the thickness of the lamella). Values of the long spacing L are presented in the last column of the table. As may readily be seen, all three sizes remain constant within experimental error. The long period also stays constant after the treatments of the samples. A slight increase in L may be seen for sample F, which, due to the high temperature of the processing steps (190 against 160°C, Table I), is exposed to more significant dephasing in the amorphous regions as shown previously for the same PEE thermoplastic elastomer.[24] It is the volume increase of the amorphous phase which contributes to the increase of the long spacing L with annealing temperature and not the lamellar thickening (as proven by WAXS and SAXS for this copolymer[25]). Also, neither does the lamellar thickness change in the present case, as can be concluded from the $D_{\bar{1}04}$ values in Table III, which are relevant to the crystal sizes in the chain direction.

WAXS measurements were performed to characterize the orientation achieved during the ZD–ZA treatment. Figure 3 shows azimuthal scans of the ($\bar{1}04$) reflection for $\chi = -36°$–$36°$ for samples A–F (Table I) and for the isothermally annealed samples G and H; χ is the azimuthal angle. For the crystallites oriented with the "c"-axis parallel to the fiber axis, the $\langle \bar{1}04 \rangle$ direction makes an angle of approximately 10° with the fiber axis, which results in two symmetrical maxima on these scans, lying at $\chi = \pm 10°$. In the case of a low degree of orientation, these maxima overlap, and as the orientation improves, they become better developed.[26]

As can be concluded from the resolution of the two maxima, samples A and D reveal good orientation, and samples B and E, a somewhat better one, while samples C and F have the best orientation. The CD–IA samples G and H reveal very good orientation, but in the latter case, the intensity is weaker, which can be explained by the existence of two fractions of PBT crystallites—the first one having very good orientation and the second one consisting of randomly oriented crystallites. This idea is further explored in the next figure. Generally, one can conclude from Figure 3 that it is the multiple

Table III Crystallite Size (D_{010}, D_{100}, $D_{\bar{1}04}$) and Long Spacing L for Samples Subjected to Either the ZD–ZA or CD–IA Treatment at Constant Length

Sample Designation	D_{010} (Å)	D_{100} (Å)	$D_{\bar{1}04}$ (Å)	L (Å)
Zone drawn–zone annealed (ZD–ZA)				
A	114	102	57	138 ± 6
B	137	115	53	134 ± 6
C	122	111	56	143 ± 7
D	132	105	54	134 ± 6
E	117	105	66	139 ± 6
F	126	125	56	162 ± 8
Cold drawn–isothermally annealed (CD–IA)				
G	116	106	54	168 ± 8
H	116	143	52	119 ± 10
				205 ± 6

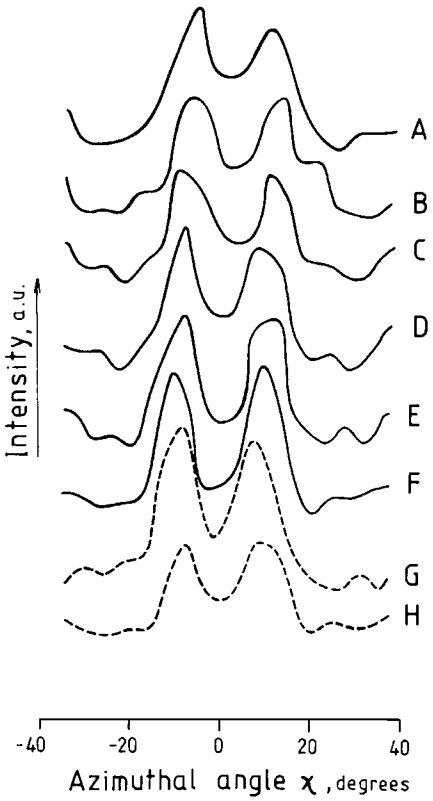

Figure 3 Azimuthal scans of the (104) reflection for the blend subjected to the ZD–ZA and CD–IA treatments. For sample designations, see Figure 1.

zone annealing at the highest load of 50 MPa (orientation step λ_3, Table I), which leads to a substantial improvement of the orientation.

Mechanical Characterization

The results of the mechanical tests on all the samples are presented in Table IV. Comparing the treatment conditions (Table I) and the data of mechanical measurements (Table IV), one can conclude that the lowest treatment temperature (160°C), resulting in the lowest final draw ratio of 4.0, is distinguished by the lowest mechanical characteristics (sample A, Table IV). If another zone annealing at the same temperature (160°C) is added to this treatment, a slightly higher draw ratio is achieved (4.4) and increase in the E and σ values is observed (sample B, Table IV).

A drastic increase in the Young's modulus (by 70% in comparison to sample A) can be obtained in the case when the second zone annealing is carried out at 190°C instead of 160°C and the highest draw ratio of 5.9 is obtained (sample C, Table IV). This combination of treatment is characterized by the highest σ value ($\sigma = 213 \pm 28$ against $\sigma = 167 \pm 4$ for sample A, Table IV).

One has to note that while a steady increase of E and σ values for these three samples is observed, the elongation at break ε systematically drops from 100 to 25% (Table IV). It seems worth noticing that all three samples (A, B, and C) are ZD at the same conditions and have the same draw ratio $\lambda_1 = 3.8$ after this treatment (Table I). It means that the significant improvement in the mechanical properties (Table IV) is achieved during the zone annealing where a higher draw ratio and, respectively, higher orientation is realized. This conclusion is supported by the second set of three samples (D, E, and F, Table I).

All three samples are ZD again at the same conditions reaching the same $\lambda_1 = 4.2$ (Table I). The subsequent zone annealing at 190°C is different for the three samples with respect to the values of stress P and number of passages N, resulting in different final draw ratios of 4.5, 4.6, and 5.2, respectively (Table I). Similarly to the first set of samples (A, B, and C), in the second one, almost the same increase in the E and σ values is observed (Table IV). What is different is the behavior of the elongation at break—it drops slightly only for sample F (Table IV).

Comparing the mechanical properties of the two sets of samples, differing mainly in the temperature of the zone drawing (Table I), a striking observation can be made—zone drawing at higher temperature (190°C instead of 160°C), followed by one-stage zone annealing at the same temperature, results in

Table IV Young's Modulus E, Tensile Strength σ, and Relative Deformation at Break ε for Samples Subjected to Either the ZD–ZA or CD–IA Treatment at Constant Length

Sample Designation	E (MPa)	σ (MPa)	ε (%)
Zone drawn–zone annealed (ZD–ZA)			
A	700 ± 40	167 ± 4	100 ± 20
B	850 ± 190	200 ± 50	39 ± 12
C	1200 ± 170	213 ± 28	25 ± 2
D	930 ± 50	185 ± 19	46 ± 10
E	1050 ± 70	195 ± 12	47 ± 7
F	1210 ± 60	202 ± 22	29 ± 6
Cold drawn–isothermally annealed (CD–IA)			
G	430 ± 70	128 ± 10	46 ± 17
H	480 ± 90	113 ± 12	50 ± 14

much lower E and σ values in comparison to the values, obtained as a result of drawing at a lower temperature and annealing at almost the same conditions (compare samples C and D, Tables I and IV). The reason for this significant difference can be related not only to the different draw ratios (λ_3 = 5.9 for sample C and 4.5 for sample D), supposing a completely different degree of orientation, but also to the higher zone-drawing temperature for sample C (190°C). At this temperature for both types of treatment, zone drawing and zone annealing (Table I), the low-melting crystallites are in a molten state (Table II) and the subsequent crystallization during the cooling takes place in isotropic conditions as proved by X-ray analysis (Fig. 4). In this way, both the low-melting crystallites and their amorphous phase contribute to the decrease of the total orientation in comparison to sample C. The multiple zone annealing at 190°C improves the mechanical properties, particularly in the case when the draw ratio increases (λ_3 = 5.2 instead of 4.5, samples F and D, Tables I and IV).

Since the treatment of the second set of samples (D, E, and F) is performed at 190°C (except the last zone annealing of sample E, Table I), one has to expect a lower degree of overall orientation in comparison to the first set of samples. For this reason, one has to look for other factors, contributing to the observed improvement, as, e.g., better adhesion between both partners of the blend.

Finally, it should be noted that the applied treatment via zone drawing and zone annealing results in significant improvement in the mechanical properties in comparison to the cold drawing and isothermal annealing with fixed ends. This can readily be seen from Table IV, which presents the data for the two approaches. Specifically, for applying the same temperatures, the zone-drawing and zone-annealing method leads to a threefold increase in the modulus E and to a twofold increase in the tensile strength σ, as well as a decrease in the relative deformation ε.

DISCUSSION

Among the results on the ZD–ZA blends of PBT and thermoplastic elastomer PEE, the most interesting are those on the mechanical properties. The improvements obtained for the Young's modulus and the tensile strength (two- to threefold) in comparison to data reported for the CD–IA blends suggests the creation of more nearly optimal structures. The values obtained in the present study for E and σ (between 1000 and 1200 MPa and ~ 200 MPa, respectively) are typical for CD–IA homo-PBT at the same treatment temperature.[7]

It is important to take into account the very poor mechanical properties of the thermoplastic elastomers. Specifically, the PEE used as a neat material (with composition PBT/PEG = 49/51 wt %) has values of E and σ of ~ 40 and 20 MPa, respectively. In blends with homo-PBT (approximately 1 : 1 by weight), the CD–IA materials show a dramatic increase in E and σ by a factor of six and 12, respectively, while the ZD–ZA materials show another two- to threefold increase in these values (Table IV). Thus, there are total increases of E and σ by factors ~ 30 and 10, respectively.

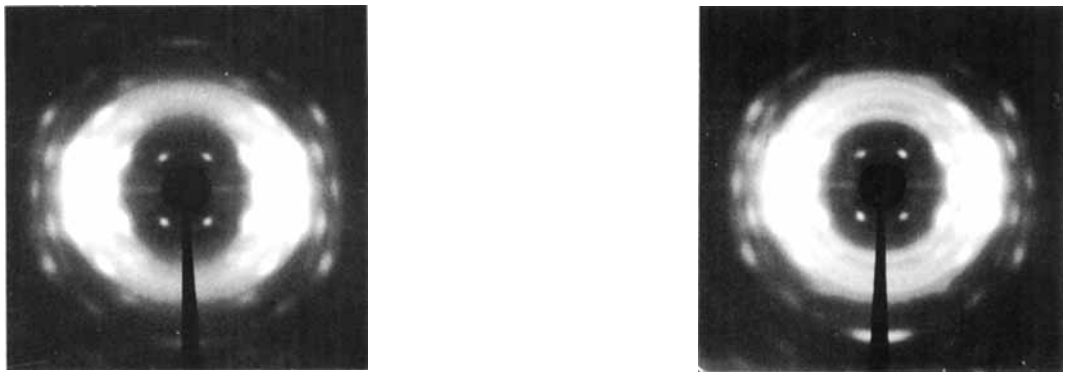

Figure 4 WAXS patterns for the blends: (a) sample A; (b) sample F. For sample designations, see Table I.

Why does the zone drawing and zone annealing contribute much more to the improvement of the mechanical properties than do cold drawing and isothermal annealing? The major factor contributing to better mechanical properties in the case of ZD–ZA is the more homogeneous structure. This conclusion is based on the DSC and particularly on the SAXS measurements shown in Figures 1 and 2 and tabulated in Tables II and III. As proved previously for the same blend,[7] CD–IA leads to the formation of two populations of crystallites having different T_m's and causing two long spacings. Both types refer to PBT crystallites but they have different origins. The less perfect crystallites arise from PEE, and the more nearly perfect ones, from homo-PBT.

In the case of the ZD–ZA blends, the tendency to form two populations of PBT crystallites is much less developed. One observes again two melting temperatures, T'_m and T''_m (Fig. 1), but no longer any occurrence of two periodicities (Fig. 2, samples A–F). Although the crystallite sizes for both methods of sample treatment do not differ from one another, the SAXS results (Fig. 2) suggest that the less perfect crystallites from the PEE are more or less homogeneously dispersed in the material and do not give rise to a second long spacing. An additional argument supporting this interpretation is their low density (approaching that of the amorphous phase), which does not seem to occur in the CD–IA blends (Fig. 2, curves G and H).

Another important factor, which can be connected with the mechanical properties, is the orientation. Although the orientation in the case of the ZD–ZA is, as a whole, not better than the orientation in the CD–IA samples, it is worth noting that the highest E value (sample F, Table IV) corresponds to the best orientation (Sample F, Fig. 3).

In the third place, one has to take into consideration the formation of microfibrillar composites when the thermal treatment above the melting temperature of less perfect crystallites is applied. (In the present case, the annealing temperature T_a = 190°C, since the lower-melting temperature T'_m is around 180°C). This effect was observed for the same blend annealed at 200°C.[7] To check the occurrence of isotropization of the crystallites originating from PEE, photographic WAXS patterns were taken for ZD–ZA samples treated either below T'_m or above T'_m. The results are displayed in Figure 4. One can see that for sample A, for which T_a does not exceed 160°C, sharp crystalline reflections in the shape of arcs are obtained. For the sample treated at 190°C (above T'_m), in addition to the arc-type reflections, one also observes reflections in the form of continuous circles, indicating the presence of an isotropic crystalline phase. It should be noted that both types of reflections arise from the PBT crystallites but with different origins and degrees of perfection. The fraction of PEE in the blend is about $\frac{1}{2}$, that of PBT in PEE is also $\frac{1}{2}$, and approximately $\frac{1}{2}$ (or less) of this PBT is in the crystalline state. (The crystallization ability in the case of the ZD–ZA materials is lower than in the CD–IA ones.) It follows that the fraction of randomly oriented crystallites in the blend is less than $\frac{1}{8}$, which explains the very weak intensity of the circles relatively to the arcs.

As shown previously,[7] the oriented crystallites must come from the homo-PBT, since the applied T_a was not high enough to melt them ($T_m \sim 225$°C, Table II). The nonoriented crystallites originate from the PEE, which during the zone annealing at 190°C is in a molten state and which during the subsequent cooling crystallizes again but no longer into an oriented state. In this way, the second component of the blend, the PEE, is in the isotropic state after this treatment, whereas the homo-PBT is in a highly oriented state.

Additional measurements indicated that for the CD–IA samples[7] the isotropic crystallization of PEE occurs on the preexisting crystallites of homo-PBT, i.e., partial cocrystallization occurs. This contributes to improvement of the adhesion between the two immiscible components of the blend (PEE and homo-PBT). There is no reason not to expect the same behavior for the ZD–ZA samples after their isotropization. The partial cocrystallization in this case could be less, because of the above-mentioned factors, leading to a poorer crystallibility of the ZD–ZA samples in comparison to the CD–IA ones. Even in such a case, the partial cocrystallization and isotropization of the PEE will contribute to improvement of the integrity of the material.

Summarizing, one has to note that as in the case of other polymers[16] the zone-drawing–zone-annealing technique applied to PBT/PEE blends results in significant improvements in their mechanical properties. The values obtained for E and σ are two- to threefold higher than those for the same blend subjected only to cold drawing and isothermal annealing at a fixed length. The values of E and σ, obtained in the present study, are equal to the mechanical parameters of homo-PBT subjected to cold drawing and isothermal annealing and higher by about 30 and 10 times, respectively, than those of the PEE used for the blending. The observed improvement is related to the more nearly optimal structure created during the zone-drawing–zone-

annealing treatment. These improvements are due to (i) more homogeneous structures, (ii) better adhesion between the components of the blend, and (iii) a somewhat better orientation. More detailed studies in the contribution of the different treatment factors (temperature duration, stress, etc.) to the improvement of the mechanical properties of the blend under investigation are in progress.

The authors gratefully acknowledge the financial support provided by the U.S. National Science Foundation, through Grant INT-9115524, as well as the support of the Bulgarian Ministry of Education and Science under Contract X-542. One of us (A. A. A.) gratefully acknowledges the hospitality of the Department of Chemistry of the University of Cincinnati where this work was completed.

REFERENCES

1. L. A. Utracki, *Polymer Alloys and Blends,* Hanser, Munich, 1989.
2. M. Fischer, in *The Interfacial Interactions in Polymeric Composites,* G. Akovali, Ed., Kluwer, Dordrecht, 1992, p. 415.
3. R. Holsti-Mettinen, J. Seppaelae, and O. T. Ikkala, *Polym. Eng. Sci.,* **32,** 868 (1992).
4. A. R. Padwa, *Polym. Eng. Sci.,* **32,** 1703 (1992).
5. M. Brown, *Rubb. Indust.,* **9,** 102 (1975).
6. K. P. Gallagher, X. Zhang, J. P. Runt, G. Huynh-ba, and J. S. Lin, *Macromolecules,* **26,** 588 (1993).
7. A. A. Apostolov, S. Fakirov, B. Sezen, I. Bahar, and A. Kloczkowski, *Polymer,* **35,** 5247 (1994).
8. A. A. Apostolov and S. Fakirov, *J. Macromol. Sci.-Phys.,* **31,** 329 (1992).
9. M. Evstatiev and S. Fakirov, *Polymer,* **33,** 877 (1992).
10. S. Fakirov, M. Evstatiev, and S. Petrovich, *Macromolecules,* **26,** 5219 (1993).
11. S. Fakirov, M. Evstatiev, and J. M. Schultz, *Polymer,* **34,** 4669 (1993).
12. S. Fakirov and M. Evstatiev, in *The Interfacial Interactions in Polymeric Composites,* G. Akovali, Ed., Kluwer, Dordrecht, 1992, p. 417.
13. S. Fakirov and M. Evstatiev, *Adv. Mater.,* **6,** 395 (1994).
14. P. J. Flory, *Principles of Polymer Chemistry,* Cornell University Press, Ithaca, NY, 1953.
15. S. Fakirov, in *Solid State Behavior of Linear Polyesters and Polyamides,* J. M. Schultz and S. Fakirov, Eds., Prentice-Hall, Englewood Cliffs, NJ, 1990, p 1.
16. T. Kunugi, in *Oriented Polymer Materials,* S. Fakirov, Ed., Huethig und Wepf Verlag, Heidelberg, 1996, p. 394.
17. A. Cifferi and M. Ward, Eds., *Ultra High Modulus Polymers,* Applied Science, London, 1979, p. 169.
18. A. Peterlin, *Colloid Polym. Sci.,* **265,** 357 (1987).
19. L. Fischer and W. Ruland, *Colloid Polym. Sci.,* **261,** 717 (1983).
20. J. Petermann and R. M. Gohil, *J. Mater. Sci.,* **14,** 2260 (1979).
21. H. Brody, *J. Macromol. Sci.-Phys. B,* **22,** 19 (1983).
22. S. Fakirov and T. Gogeva, *Makromol. Chem.,* **191,** 603 (1990).
23. V. P. Privalko, *Handbook on Physical Chemistry of Polymers,* Vol. 2, Naukowa Dumka, Kiev, 1984 (In Russian).
24. S. Fakirov, A. A. Apostolov, P. Boeseke, and H. G. Zachmann, *J. Macromol. Sci.-Phys. B,* **29,** 379 (1990).
25. S. Fakirov, A. A. Apostolov, and C. Fakirov, *Int. J. Polym. Mater.,* **18,** 51 (1992).
26. L. E. Alexander, *X-Ray Diffraction Methods in Polymer Science,* Wiley-Interscience, New York, 1969, p. 262.

Received March 13, 1995
Accepted August 28, 1995